Electronic Supplementary Information (ESI):

Ratiometric detection of amyloid-β aggregation by a dual-emissive tris-heteroleptic ruthenium complex

Jiang-Yang Shao,[a,b] Si-Hai Wu,*[a] Junjie Ma,[a] Zhong-Liang Gong,[b] Tian-Ge Sun,[b] Yulong Jin,[b] Rong Yang,[a] Bin Sun,[c] and Yu-Wu Zhong*[b,d]

[a] School of Medicine, Huaqiao University, Quanzhou, Fujian 362021, China

[b] Beijing National Laboratory for Molecular Sciences, CAS Key Laboratory of Photochemistry, CAS Research/Education Center for Excellence in Molecular Sciences, Institute of Chemistry, Chinese Academy of Sciences, Beijing 100190, China

[c] Institute of BioPharmaceutical Research, Liaocheng University, Liaocheng 252000, China

[d] School of Chemical Sciences, University of Chinese Academy of Sciences, Beijing 100049, China

*Email: wusihai@hqu.edu.cn (S.-H.W.); zhongyuwu@iccas.ac.cn (Y.-W.Z.)

Synthesis and Characterization

General. NMR spectra were recorded in the designated solvent on a Bruker Avance spectrometer. Spectra are reported in ppm values from residual protons of the deuterated solvent. Mass data were obtained with a Bruker Daltonics Inc. Apex II FT-ICR or Autoflex III MALDI-TOF mass spectrometer. The matrix for MALDI-TOF measurement is α-cyano-4-hydroxycinnamic acid. Microanalysis was carried out using a Flash EA 1112 or Carlo Erba 1106 analyzer at the Institute of Chemistry, Chinese Academy of Sciences.
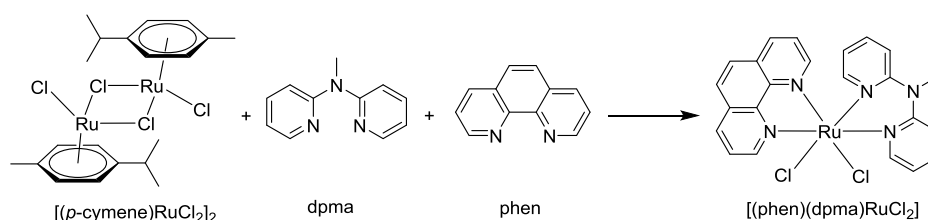
Synthesis of the Intermediate Complex [(phen)(dpma)RuCl₂]. A solution of dichloro(*p*-cymene)ruthenium(II) dimer (61.2 mg, 0.10 mmol) and *N*,*N*-di(pyrid-2-yl)-methylamine (dpma, 36.0 mg, 0.20 mmol) in 10 mL of DMF was heated at 85 °C for 5 h under N_2 atmosphere, followed by the addition of 37.0 mg of 1,10-phenanthroline (phen, 0.20 mmol). The resulting mixture was heated for another 4 h at 140 °C. After cooling to room temperature, DMF was removed under vacuum. To the residue was added 30 mL of acetone. The solution was cooled at –25 °C overnight. The resulting precipitate was collected and washed with several portions of ethanol, water and diethyl ether to give 95 mg of [(phen)(dpma)RuCl₂] as a deep purple solid in 89% yield. This crude product was used for next transformation without further purification. MALDI-MS (m/z): 501.7 for $[M - Cl]^+$. ESI-MS (m/z) calcu 502.0417 for $C_{23}H_{19}ClN_5Ru$, $[M - Cl]^+$; found: 502.0 (Figure S16).
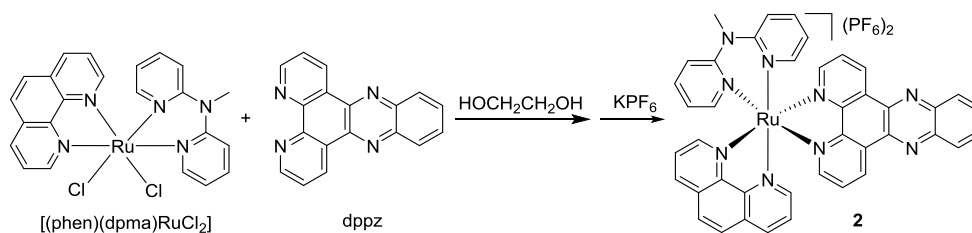
Synthesis of Complex 2. To a solution of the above prepared intermediate [(phen)(dpma)RuCl$_2$] (53.7 mg, 0.10 mmol) in 8 mL of ethylene glycol was added ligand dppz (28.2 mg, 0.10 mmol). The resulting mixture was heated under microwave irradiation for 0.5 h (power = 325 W). After cooling to room temperature, an excess of an aqueous solution of KPF$_6$ was added. The resulting precipitate was collected and purified by flash column chromatography on silica gel using CH$_2$Cl$_2$/CH$_3$CN (5/1) as the eluent to give 85 mg of **2** as an orange solid in 83% yield. ^{1}H NMR (400 MHz, CD$_3$CN): δ 3.52 (s, 3H), 6.74 (q, J = 8.0 Hz, 2H), 7.38-7.51 (m, 4H), 7.55-7.61 (m, 2H), 7.79-7.84 (m, 3H), 7.96 (d, J = 4.0 Hz, 1H), 8.00 (dd, J = 5.2 Hz and 2.8 Hz, 1H), 8.10-8.19 (m, 4H), 8.28 (d, J = 8.0 Hz, 1H), 8.42-8.51 (m, 3H), 8.76 (d, J = 8.0 Hz, 1H), 8.89 (dd, J = 5.2 Hz and 3.6 Hz, 2H), 9.47 (d, J = 8.0 Hz, 1H), 9.78 (d, J = 8.0 Hz, 1H). ^{13}C NMR (100 MHz, CD$_3$CN): δ 40.4, 116.2, 116.3, 120.6, 125.6, 125.7, 126.8, 126.9, 127.9, 128.2, 129.6, 130.8, 131.0, 131.3, 132.5, 132.9, 133.7, 136.4, 137.2, 139.3, 139.4, 140.1, 140.2, 142.7, 147.9, 148.2, 151.0, 151.2, 153.1, 154.1, 155.0, 158.1, 158.2. MALDI-MS (m/z): 752.2 for [M − 2PF$_6$ − 3]$^+$. Anal. Calcd. for C$_{41}$H$_{29}$F$_{12}$N$_9$P$_2$Ru: C, 47.41; H, 2.81; N, 12.14. Found: C, 47.26; H, 2.95; N, 11.82.

HPLC Analysis

HPLC analysis was performed on a Shimadzu UFLC system consisting of two LC-20AD pumps, a SPD-M20A diode array detector, a CTO-20A oven, and a SIL-20A autosampler. HLPC grade solvents were obtained from Fisher Scientific. A Shim-pack XR-ODS (Shimadzu, Japan) column (2.2 μm, 75 mm × 4.6 mm, i.d.) was used for the analysis. Compounds were eluted with a gradient solvent of CH$_3$CN in water (10 - 90% over 0 - 10 min), followed by isocratic elution of 90% CH$_3$CN for 5

min. All solvents contain 0.1% of trifluoroacetic acid (TFA). The flow rate was 1.0 mL/min. The detection wavelengths were set at 322 nm and 410 nm for ligand dpma and complex **2**, respectively.

Preparation and Analysis of Aβ fibril

Methods for fibril preparation and assay were adapted from Bieschke *et al.* and Fezoui *et al.*[1] High purity Aβ$_{40}$ (99.8%) and Aβ$_{42}$ (98.5%) were purchased from ApexBio Tech LLC. A basic stock solution of monomeric Aβ was prepared by adding 300 μL of 25 mM aqueous NaOH to 1 mg of Aβ, followed by sonication for 2 min. The solution was filtered through 0.2 μm centrifuge filter. The filtrate was diluted with buffer (300 mM NaCl/100 mM Tris, pH = 7.5) to a final volume of 1 mL and stored in refrigerator. The Aβ concentration was determined using a UV-visible spectrophotometer at λ of 280 nm (ε = 1280 M^{-1}cm^{-1}). The freshly prepared Aβ solution was incubated at 37 °C and 700 rpm using a BL-100A thermo shaker. After certain incubation duration, to the sample was added an equivalent amount of photoluminescent probe (complex **2** or ThT) and the mixture was analyzed by the spectrofluorimeter.

Spectroscopic Analysis

All optical absorption spectra were obtained using a TU-1810DSPC spectrometer of Beijing Purkinje General Instrument Co. Ltd. at room temperature in denoted solvents, with a conventional 1.0 cm quartz cell. Emission spectra were recorded using a F-380 spectrofluorimeter of Tianjin Gangdong Sic. & Tech Development Co. Ltd, with a red-sensitive photomultiplier tube R928F. Samples for emission measurement were obtained within quartz cuvettes of 1 cm path length. Luminescence quantum yields were determined using quinine sulfate in 1.0 M aq H$_2$SO$_4$ (Φ = 55%) or [Ru(bpy)$_3$](PF$_6$)$_2$ (Φ = 9.5%) in degassed acetonitrile solution as the standard; estimated uncertainty of ϕ is ±10% or better.

Emission Lifetime Analysis

The luminescence decays were measured using a nanosecond flash photolysis setup Edinburgh FLS920 spectrometer (Edinburgh Instruments Ltd.), combined with a picosecond pulsed diode laser. A monochromator equipped with a photomultiplier for collecting the spectral range from 300 to 850 nm was used to analyze the luminescence decays. Data were analyzed by the online software of the FLS920 spectrophotometer.

Time-Resolved Photoluminescence Measurements

Nanosecond time-resolved photoluminescence (TRPL) spectra were measured using a nanosecond flash photolysis setup Edinburgh LP920 spectrometer (Edinburgh Instruments Ltd.), combined with a Nd:YAG laser (Surelite II, Continuum Inc.). The sample was excited by a 375 nm pulsed laser. A monochromator equipped with a photomultiplier for collecting the spectral range from 400 to 900 nm. Data were analyzed by the online software of the LP920 spectrophotometer.

DFT and TDDFT Calculations

DFT calculations were carried out by using the B3LYP exchange correlation functional[2] and implemented in the Gaussian 09 package.[3] The electronic structures were optimized with a general basis set with the Los Alamos effective core potential LANL2DZ basis set for Ru and 6-31G* for other atoms.[4] The solvation effects in CH_3CN were included for all calculations. No symmetry constraints were used in the optimization (nosymm keyword was used). Frequency calculations were performed with the same level of theory to ensure the optimized geometries to be local minima. All orbitals were computed at an isovalue of 0.03 e bohr^{-3}. TDDFT calculations were performed on the DFT-optimized structures on the same level of theory.

Transmission Electron Microscopy

Samples were prepared by drop-casting the fibril solutions on 300 mesh ultra-thin carbon film with 3% uranyl acetate as a negative stain. The measurements were

performed on a FEI Tecnai G2 F20 S-Twin high-resolution transmission electron microscope under an acceleration voltage of 200 kV.

Molecular Docking Calculations

Molecular docking study was carried out by using the Discovery Studio 3.5 software package. The $A\beta_{40}$ fibril structure (PDB ID: 2LMO) was retrieved from the RCSB Protein Data Bank as the receptor. The $A\beta_{40}$ fibril structure was prepared by adding hydrogen atoms, removing water molecules and assigning Charmm force field. The sphere including residues Val18 and Phe20 were defined as the binding site.[5] The parameter of active sphere was set to 9 Å. Then, the target compounds were docked into the active site using CDOCKER program. The pose cluster radius and random conformations were set to 10, and all other options remain the default during the parameter setting. Libdock program was carried out to obtain the docking results. In the amino acid mutation module, the key amino acid residue Val 18, Phe20, and Glu22 was mutated to Ala18, Ser20, and Arg22, respectively.

Confocal Laser Scanning Microscopy (CLSM)

CLSM was performed using OLYMPUS FV3000-IX81 confocal microscope (Olympus Corporation, Japan) with 100 × objective oil lens. Under excitation by a 488 nm laser, the confocal images of Aβ fibrils were collected at 620-720 nm and processed by Olympus FV31S-SW viewer software.
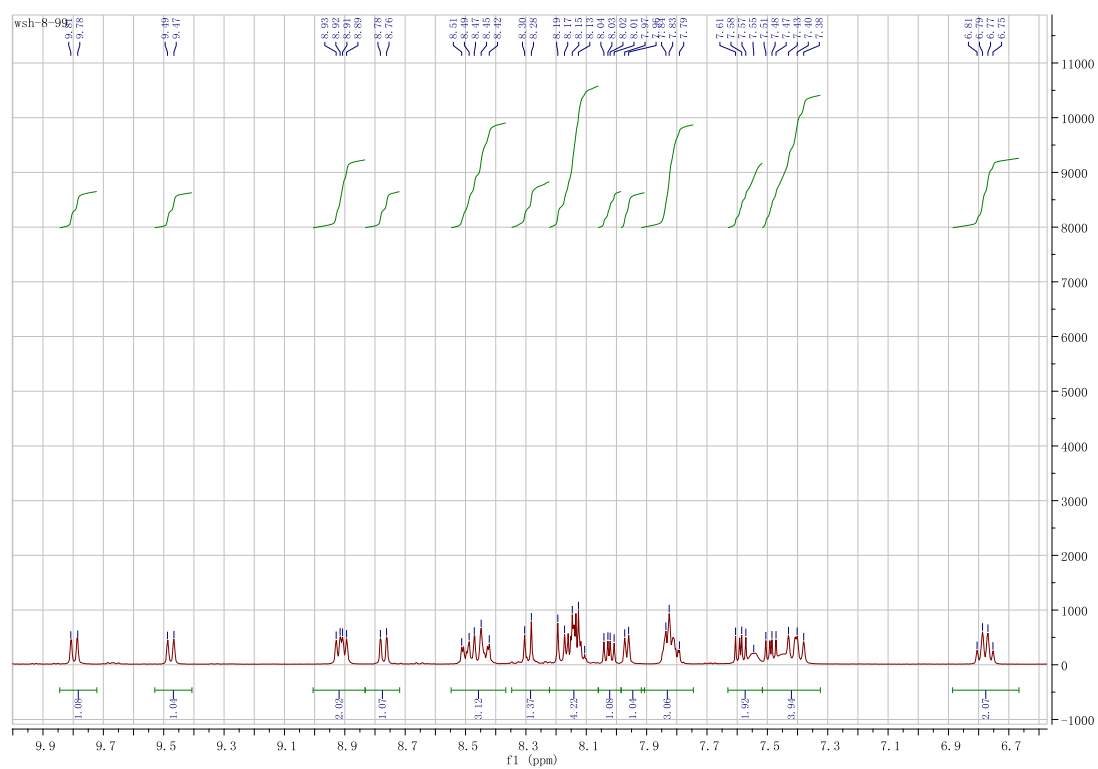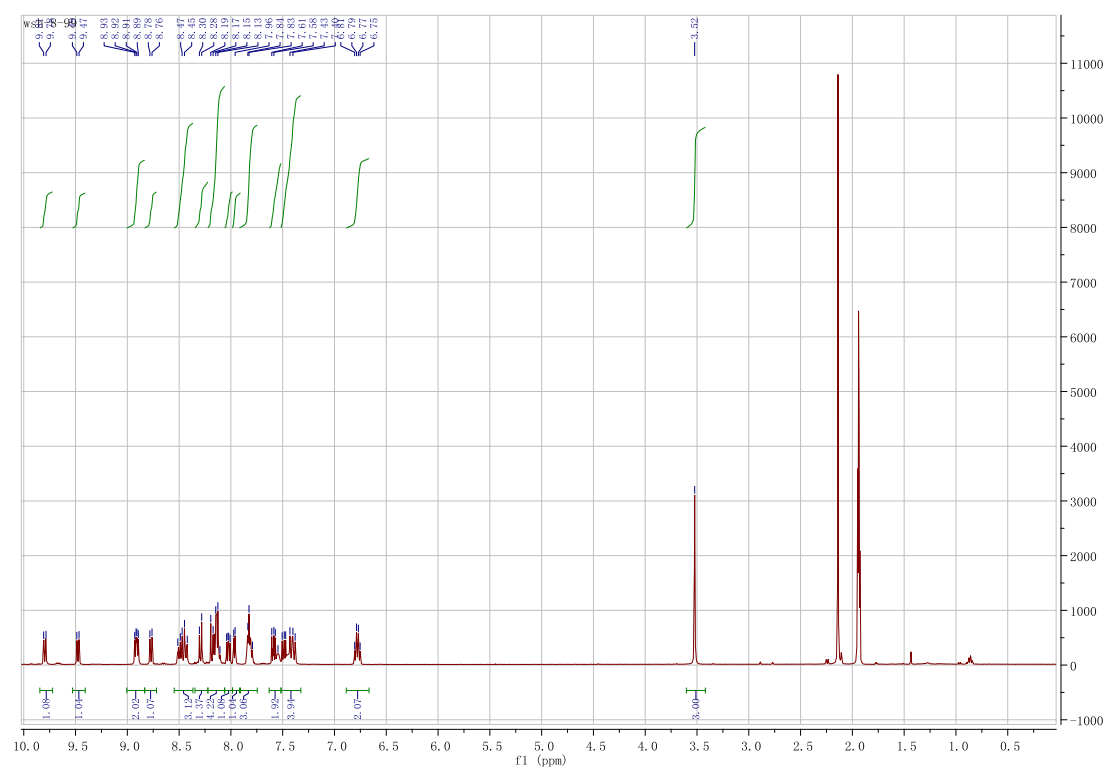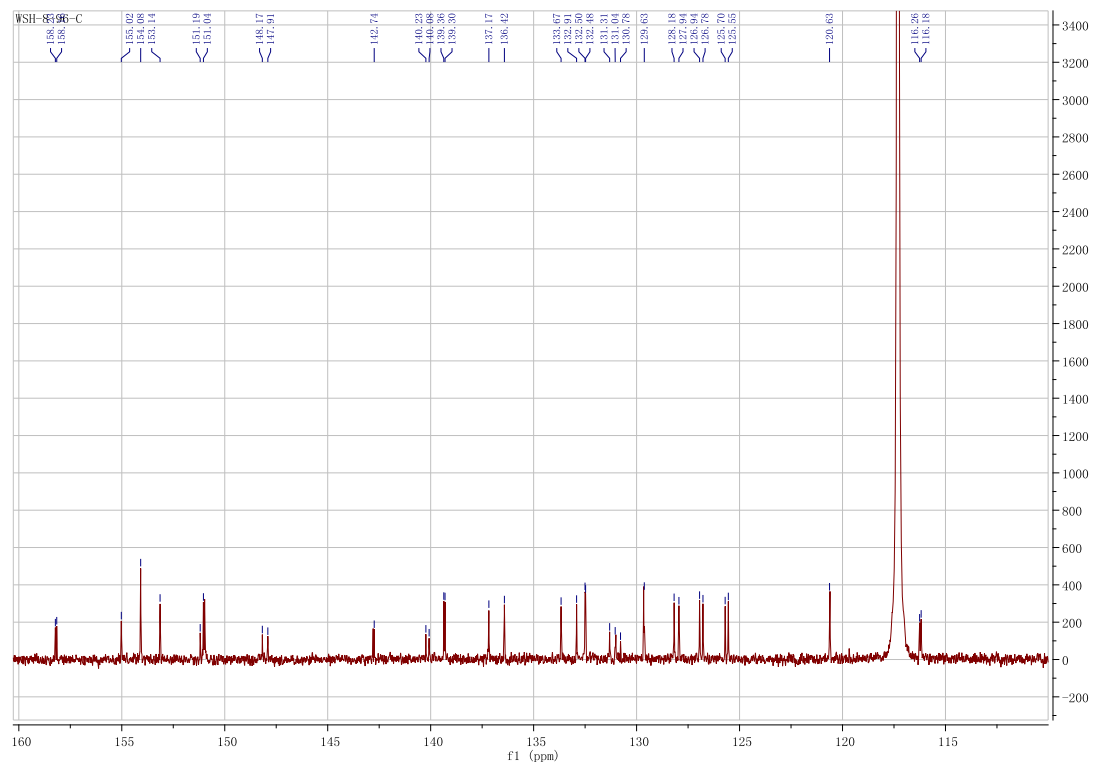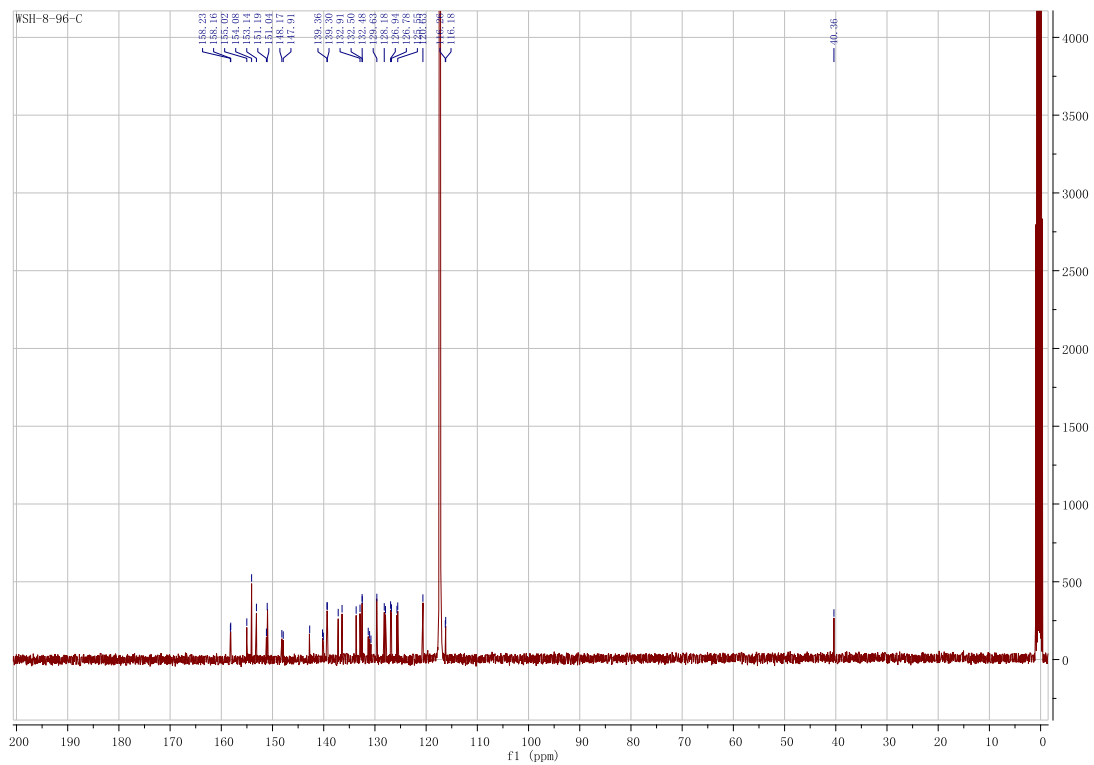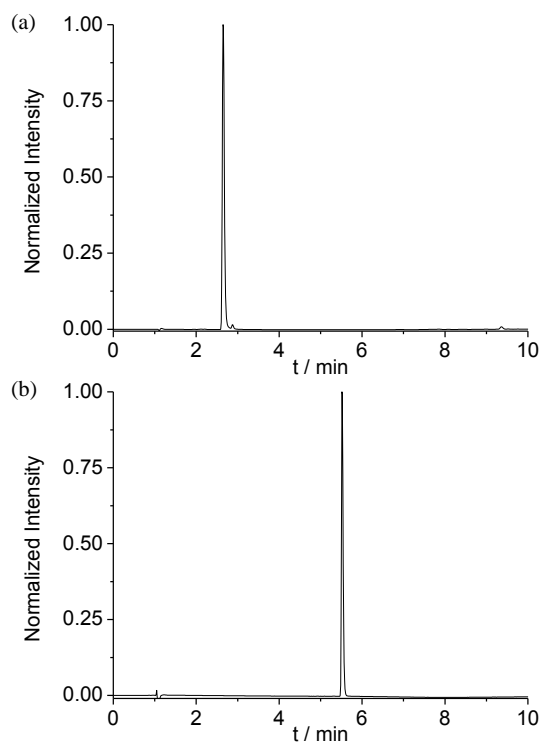
Figure S1. ^{1}H NMR spectrum of **2** in CD$_3$CN.

**Figure S2**. ^{13}C NMR spectrum of **2** in CD$_3$CN.

**Figure S3**. Analytic HPLC spectra of (a) the ligand dpma (99.03% purity) and (b) complex **2** (99.95% purity).

Table S1 Absorption and emission data.[a]

| Comp.	Solvent	$\lambda_{abs(max)}/nm$ $(\varepsilon/10^5\,M^{-1}cm^{-1})$	$\lambda_{em(max)}$[b] [nm]	τ [ns] at 77 K	τ [ns] at rt	Φ[c] at rt
dpma	CH$_3$CN	276 (0.08), 306 (0.11)	385	ND	ND	0.8%
2	CH$_3$CN	266 (0.91), 274 (0.89), 316 (0.20), 358 (0.16), 368 (0.16), 410 (0.13), 470 (0.11)	400/650	2.2/2160	4.0/261	7.3%
	buffer	266 (0.68), 274 (0.65), 360 (0.14), 372 (0.15), 410 (0.10), 470 (0.08)	415	ND	7.2	0.05%

[a]All spectra were recorded in a conventional 1.0 cm quartz cell. ND = not determined. [b]The excitation wavelength is 300 nm for ligand dpma and 330 nm for complex **2**. [c]Quantum yields were determined by comparing with quinine sulfate in 1.0 M aq. H$_2$SO$_4$ (for dpma) or [Ru(bpy)$_3$](PF$_6$)$_2$ (for **2**).
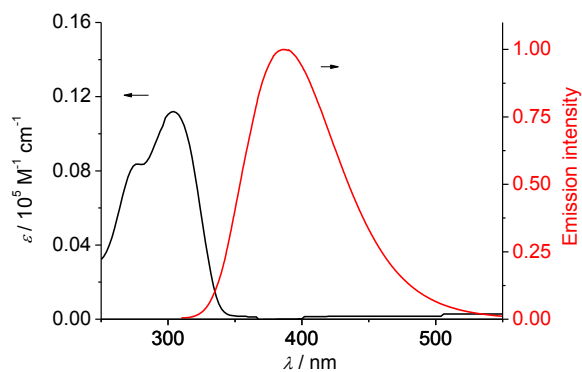
Figure S4. Absorption and emission spectra ($\lambda_{ex} = 300$ nm) of dpma in CH$_3$CN.

HOMO LUMO
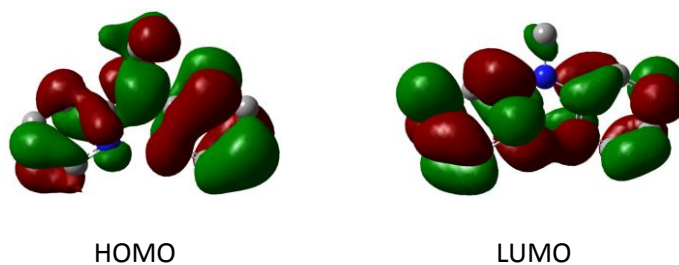
Figure S5. Isodensity plots of the HOMO and LUMO of ligand dpma. All orbitals were computed at an isovalue of 0.03.

LUMO+6 LUMO+5 LUMO+4 LUMO+3

LUMO+2 LUMO+1 LUMO HOMO

HOMO-1 HOMO-2 HOMO-3 HOMO-5
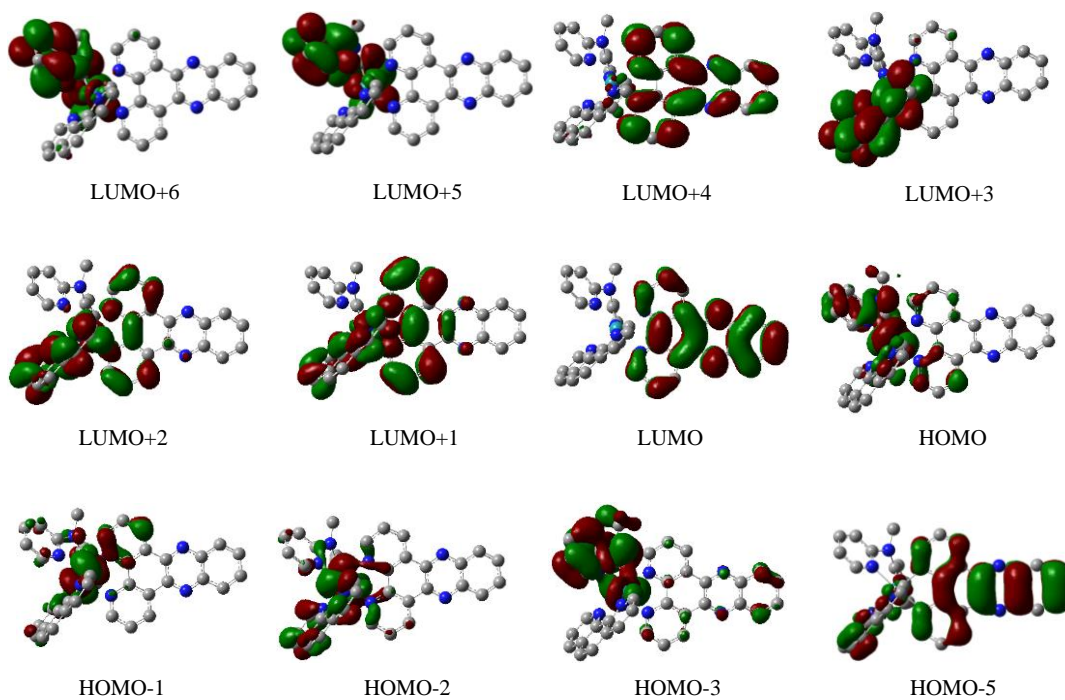
Figure S6. Isodensity plots of frontier molecular orbitals of 2^{2+}. All orbitals were computed at an isovalue of 0.03.
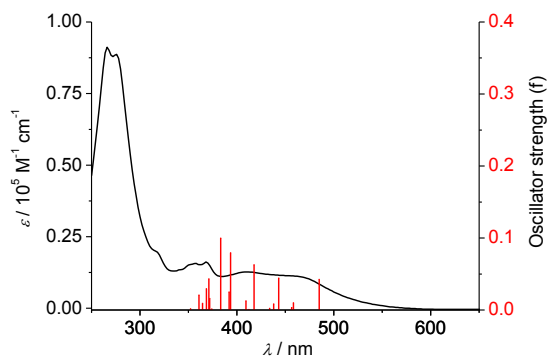
Figure S7. TDDFT-predicted excitations (red lines) and absorption spectra (black curves) of 2^{2+}.

Table S2. TDDFT results of 2^{2+}.

| S_n	E [ev]	λ [nm]	f	Dominant transition(s) (percentage contribution)	assignment
1	2.56	485	0.0427	HOMO → LUMO (85%)	$ML_{dppz}CT$; $L_{dpma}L_{dppz}CT$
4	2.80	443	0.0444	HOMO-1 → LUMO (23%)	$ML_{dppz}CT$
				HOMO → LUMO+1 (37%)	$ML_{phen}CT$; $L_{dpma}L_{phen}CT$
7	2.97	418	0.0629	HOMO-1 → LUMO+1 (48%)	$ML_{phen}CT$
10	3.15	393	0.0795	HOMO-2 → LUMO+2 (19%)	$ML_{dppz}CT$
				HOMO-1 → LUMO+3 (28%)	$ML_{phen}CT$
				HOMO → LUMO+4 (24%)	$ML_{dppz}CT$
11	3.16	392	0.0251	HOMO → LUMO+4 (64%)	$ML_{dppz}CT$
15	3.34	371	0.0433	HOMO-2 → LUMO+3 (52%)	$ML_{phen}CT$
16	3.36	369	0.0297	HOMO-3 → LUMO (36%)	$L_{dpma}L_{dppz}CT$
				HOMO-1 → LUMO+4 (39%)	$ML_{dppz}CT$
18	3.44	361	0.0208	HOMO-2 → LUMO+4 (91%)	$ML_{dppz}CT$
22	3.63	341	0.0235	HOMO-3 → LUMO+1 (16%)	$L_{dpma}L_{dppz}CT$
				HOMO-2 → LUMO+13 (15%)	$L_{dpma}L_{phen}CT$
				HOMO → LUMO+14 (15%)	$IL_{phen}CT$
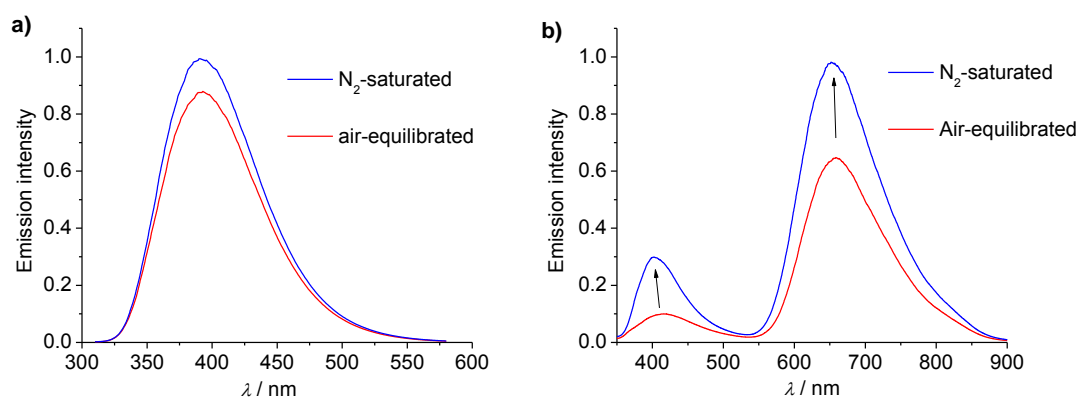
Figure S8. Emission spectra of (a) ligand dpma (λ_{ex} = 300 nm) and (b) complex **2** (λ_{ex} = 330 nm) in air-equilibrated (red curve) or N_2-saturated (blue curve) CH_3CN (1×10^{-5} M).
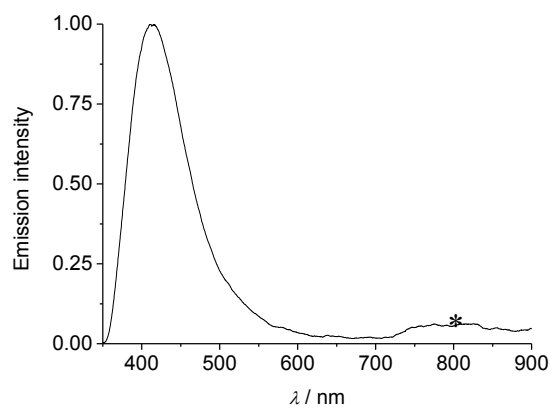
Figure S9. Emission spectrum of **2** in aqueous buffer solution (30 mM NaCl/10 mM Tris, pH = 7.5) excited at 330 nm. ∗: Artifacts from the background noise of the equipment.
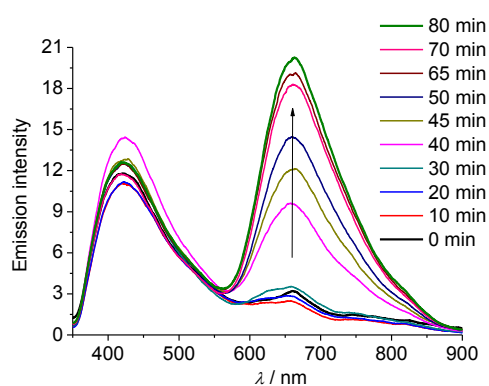

Figure S10. (a) Emission spectral changes of the mixture of **2** (14 μM) and Aβ_{40} (14 μM) after different incubation time in aqueous buffer solution (30 mM NaCl/10 mM Tris, pH = 7.5). The excitation wavelength is 330 nm.
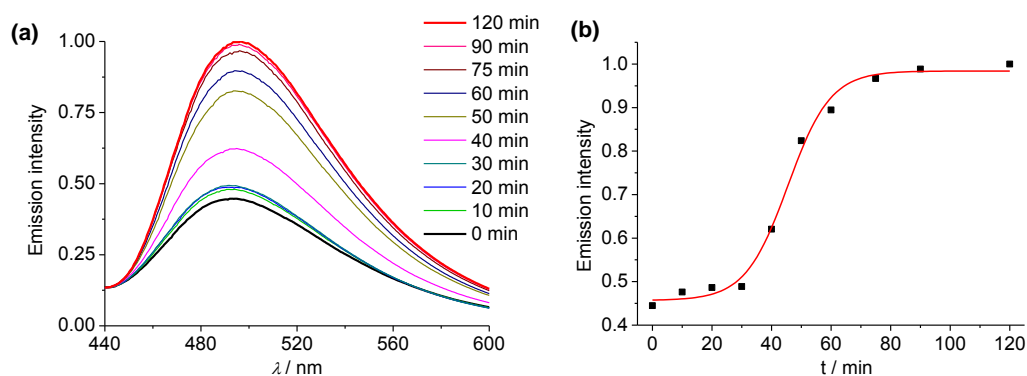
**Figure S11.** (a) Emission spectral changes monitored by Thioflavin T (14 μM) of Aβ_{40} aggregation after different incubation time in aqueous buffer solution (14 μM Aβ_{40} in 30 mM NaCl/10 mM Tris, pH = 7.5). (b) Corresponding changes of the emission intensity at 490 nm. The excitation wavelength is 420 nm.
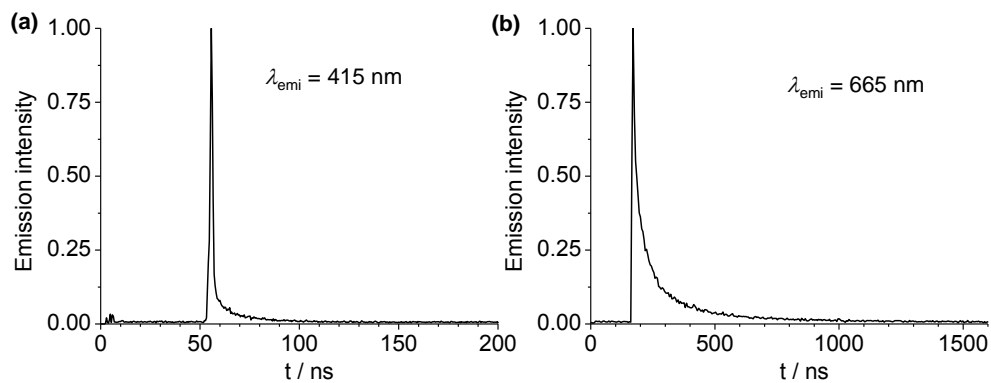
Figure S12. Decay profile of the emission intensity at (a) 415 nm and (b) 655 nm of the mixture of **2** (14 μM) and Aβ_{40} fibril (14 μM) at rt (air-equilibrated). The excitation wavelength is 330 nm.
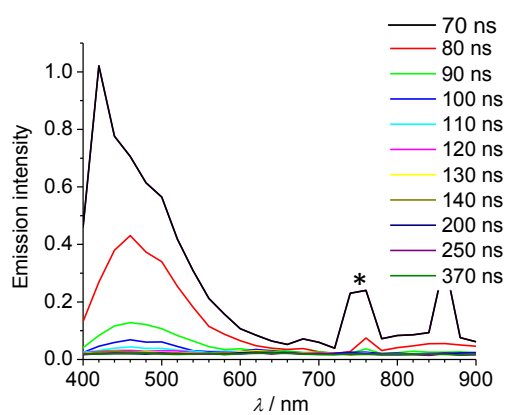

Figure S13. Time-resolved emission spectra of the mixture of **2** with free Aβ_{40} peptide (excited by a 375 nm pulsed laser). *: Second-order bands of the excitation wavelength. The instrument response time is around 70 ns.
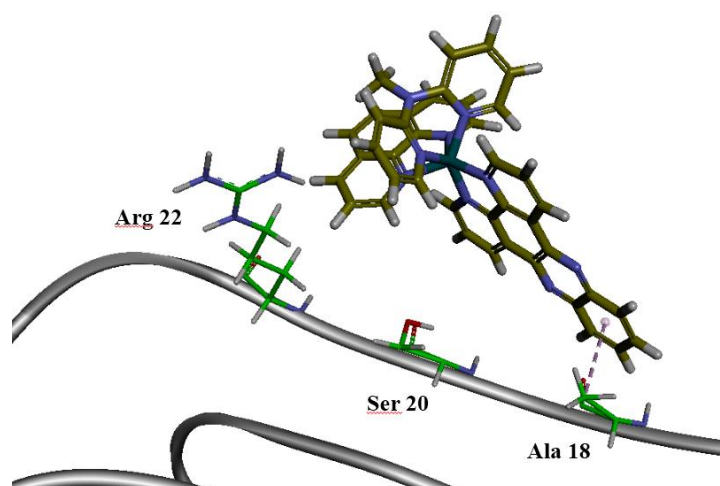
Figure S14. Molecular modeling of complex **2** with a control peptide with the key amino acid residues Val18, Phe20, and Glu22 of Aβ_{40} being mutated to Ala18, Ser20, and Arg22, respectively. The results show that the docking between **2** and the control peptide is loose, in which only the C-H/π interactions between Ala18 and dppz is observed.
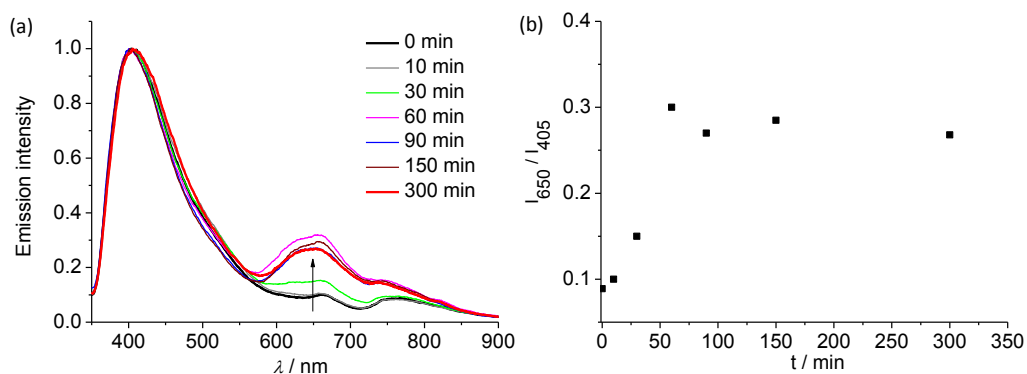
Figure S15. (a) Emission spectral changes (normalized to the emission at 405 nm) monitored by complex **2** (14 μM) of Aβ_{42} aggregation (14 μM) after different incubation time (10, 30, 60, 90, 150, 300 min) in aqueous buffer solution (excited at 330 nm). (b) Corresponding changes of the emission intensity ratio between 650 and 405 nm (I_{650}/I_{405}) of panel (a) versus incubation time.
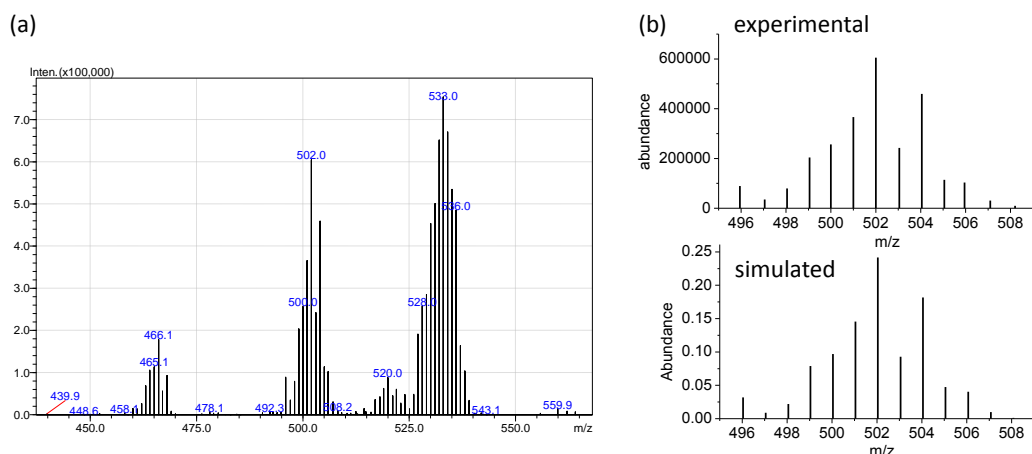
Figure S16. (a) ESI mass spectrum of the Intermediate Complex [(phen)(dpma)RuCl$_2$]. (a) A comparison of the experimental and simulated isotopic distribution of the peak at 502.0.

Reference:

1 (a) J. Bieschke, Q. Zhang, E. T. Powers, R. A. Lerner and J. W. Kelly, *Biochem.*, 2005, **44**, 4977-4983; (b) Y. Fezoui, D. M. Hartley, J. D. Harper, R. Khurana, D. M. Walsh, M. M. Condron, D. J. Selkoe, P. T. Jr. Lansbury, A. L. Fink and D. B. Teplow, *Amyloid*, 2000, **7**, 166-178.

2 C. Lee, W. Yang and R. G. Parr, *Phys. Rev. B*, 1988, **37**, 785-789.

3 M. J. Frisch, G. W. Trucks, H. B. Schlegel, G. E. Scuseria, M. A. Robb, J. R. Cheeseman, J. A. Montgomery, Jr. T. Vreven, K. N. Kudin, J. C. Burant, J. M. Millam, S. S. Iyengar, J. Tomasi, V. Barone, B. Mennucci, M. Cossi, G. Scalmani, N. Rega, G. A. Petersson, H. Nakatsuji, M. Hada, M. Ehara, K. Toyota, R. Fukuda, J. Hasegawa, M. Ishida, T. Nakajima, Y. Honda, O. Kitao, H. Nakai, M. Klene, X. Li, J. E. Knox, H. P. Hratchian, J. B. Cross, C. Adamo, J. Jaramillo, R. Gomperts, R.

E. Stratmann, O. Yazyev, A. J. Austin, R. Cammi, C. Pomelli, J. W. Ochterski, P. Y. Ayala, K. Morokuma, G. A. Voth, P. Salvador, J. J. Dannenberg, V. G. Zakrzewski, S. Dapprich, A. D. Daniels, M. C. Strain, O. Farkas, D. K. Malick, A. D. Rabuck, K. Raghavachari, J. B. Foresman, J. V. Ortiz, Q. Cui, A. G. Baboul, S. Clifford, J. Cioslowski, B. B. Stefanov, G. Liu, A. Liashenko, P. Piskorz, I. Komaromi, R. L. Martin, D. J. Fox, T. Keith, M. A. Al-Laham, C. Y. Peng, A. Nanayakkara, M. Challacombe, P. M. W. Gill, B. Johnson, W. Chen, M. W. Wong, C. Gonzalez and J. A. Pople, Gaussian 09, revision A.2; Gaussian, Inc.: Wallingford CT, 2009.

4 (a) T. H. Dunning and P. J. Hay, In *Modern Theoretical Chemistry*; Schaefer, H. F., Ed.; Plenum: New York, 1976; Vol. 3, p 1. (b) P. J. Hay and W. R. Wadt, *J. Chem. Phys.*, 1985, **82**, 299-310.

5 N. P. Cook, M. Ozbil, C. Katsamples, R. Prabhakar and A. A. Mart í *J. Am. Chem. Soc.*, 2013, **135**, 10810-10816.